Pharmacological Characterization of Ligands at Recombinant NMDA Receptor Subtypes by Electrophysiological Recordings and Intracellular Calcium Measurements

Kasper B. Hansen[*,1,2], Hans Bräuner-Osborne[1] and Jan Egebjerg[2]

[1]*Department of Medicinal Chemistry, Faculty of Pharmaceutical Sciences, University of Copenhagen, Copenhagen, Denmark*

[2]*Department of Molecular Biology, H. Lundbeck A/S, Copenhagen, Denmark*

Abstract: Generation of *in vitro* cellular assays using fluorescence measurements at heterologously expressed NMDA receptors would speed up the process of ligand characterization and enable high-throughput screening. The major drawback to the development of such assays is the cytotoxicity caused by Ca^{2+}-flux into the cell *via* NMDA receptors upon prolonged activation by agonists present in the culture medium. In the present study, we established four cell lines with stable expression of NMDA receptor subtypes NR1/NR2A, NR1/NR2B, NR1/NR2C, or NR1/NR2D in BHK-21 cells. To assess the usefulness of the stable cell lines in conjunction with intracellular calcium ($[Ca^{2+}]_i$) measurements for evaluation of NMDA receptor pharmacology, several ligands were characterized using this method. The results were compared to parallel data obtained by electrophysiological recordings at NMDA receptors expressed in *Xenopus* oocytes. This comparison showed that agonist potencies determined by $[Ca^{2+}]_i$ measurements and electrophysiological recordings correlated well, meaning that the stable cell lines in conjunction with $[Ca^{2+}]_i$ measurements provide a useful tool for characterization of NMDA receptor ligands. The agonist series of conformationally constrained glutamate analogues (2S,3R,4S)-α-(carboxycyclopropyl)glycine (CCG), 1-aminocyclobutane-r-1,cis-3-dicarboxylic acid (trans-ACBD), and (±)-1-aminocyclopentane-r-1,cis-3-dicarboxylic acid (cis-ACPD), as well as the highly potent agonist tetrazolylglycine were among the characterized ligands that were assessed with respect to subtype selectivity at NMDA receptors. However, none of the characterized agonists displays more than 2-3 fold selectivity towards a specific NMDA receptor subtype. Thus, the present study provides a broad pharmacological characterization of structurally diverse ligands at recombinant NMDA receptor subtypes.

Keywords: NMDA receptors, stable expression, FLIPR, intracellular calcium measurements, ligand characterization, Fluo-4, *Xenopus* oocytes, electrophysiology.

INTRODUCTION

N-methyl-D-aspartate (NMDA) receptors are ligand-gated cation-selective ion channels and members of the family of ionotropic glutamate receptors [1]. They are expressed throughout the mammalian central nervous system and under normal conditions, they are essential to processes as diverse as neural development, perception of pain, and synaptic plasticity including long-term depression and long-term potentiation, which are believed to form the molecular basis for memory and learning [1]. However, NMDA receptors are also implicated in several neuropathological conditions, such as ischemia, epilepsy, schizophrenia, chronic pain, and Alzheimer's disease, and they have therefore gained considerable interest as targets in the development of therapeutic agents [2].

Seven NMDA receptor subunits have been identified, namely the NR1 subunit, four NR2 subunits (NR2A-D), and two NR3 subunits (NR3A-B) [1, 3]. Functional NMDA receptors are heteromeric assemblies of two NR1 subunits and two NR2 subunits that are activated by simultaneous binding of glutamate and glycine. The NR1 subunits provide the glycine binding sites and the NR2 subunits form the glutamate binding sites [1]. Expression of the NR1 subunit alone in heterologous cells will not produce functional homomeric glycine-responsive receptors [4], and expression of the NR2 subunit alone will not produce functional homomeric glutamate-responsive receptors [5].

Cell lines stably expressing the different NMDA receptor subtypes make a solid basis for assays to efficiently determine the pharmacological properties and subtype selectivity of NMDA receptor agonists and antagonists. Several groups have described approaches to generate cell lines with stable expression of human [6-9], mouse [10] or rat [11-13] NMDA receptors. In conjunction to the cell lines, some of these studies have developed functional assays using intracellular calcium ($[Ca^{2+}]_i$) measurements [9-13]. However, none of these cell lines has been used to characterize more than two agonists at recombinant NMDA receptors using intracellular calcium ($[Ca^{2+}]_i$) measurements. It therefore remains to be shown whether stable cell lines in conjunction with $[Ca^{2+}]_i$ measurements can be used for evaluation of NMDA receptor pharmacology.

Expression of recombinant NMDA receptors in non-neuronal cell lines is associated with cytotoxicity due to

*Address correspondence to this author at the Department of Medicinal Chemistry, Faculty of Pharmaceutical Sciences, University of Copenhagen, Universitetsparken 2, DK-2100 Copenhagen, Denmark; Tel: (+45) 36 33 65 62; Fax: (+45) 36 33 60 40; E-mail: kbh@farma.ku.dk

1386-2073/08 $55.00+.00

NMDA receptor-mediated Ca^{2+}-influx induced by prolonged activation by glutamate and glycine present in the culture medium [14, 15]. Culturing the cells in the presence of NMDA receptor antagonists will partly overcome this obstacle, and generation of stable cell lines with inducible expression of NMDA receptors will further attenuate the NMDA receptor-mediated cell death [7, 8, 10-13].

In the present study, we describe cell lines with stable expression of rat NMDA receptor subtypes NR1/NR2A, NR1/NR2B, NR1/NR2C, or NR1/NR2D in BHK-21 cells. In addition, we develop an assay using $[Ca^{2+}]_i$ measurements for characterization of ligands at the stably expressed NMDA receptors. By characterizing a number of agonists, we demonstrate that the assay using $[Ca^{2+}]_i$ measurements reliably reports both potencies and relative maximal responses when comparing with data obtained by two-electrode voltage-clamp (TEVC) recordings at NMDA receptors expressed in *Xenopus* oocytes.

MATERIALS AND METHODS

NMDA receptor ligands. (S)-Glutamic acid (glutamate), (S)-aspartic acid (aspartate), (2S,3R,4S)-α-(carboxycyclopropyl)glycine (CCG), (R,S)-2-amino-5-phosphonopentanoic acid (AP5), 5,7-dichlorokynurenic acid (DCKA), memantine, MK-801, NMDA, phencyclidine (PCP), ifenprodil, and glycine were obtained from Sigma-Aldrich (Munich, Germany). (R,S)-Ibotenic acid (ibo), 1-aminocyclobutane-r-1,cis-3-dicarboxylic acid (trans-ACBD), (±)-1-aminocyclopentane-r-1,cis-3-dicarboxylic acid (cis-ACPD), (R)-4-(3-phosphonopropyl)piperazine-2-carboxylic acid (CPP), LY235959, and homoquinolinic acid (HQ), (R,S)-(tetrazol-5-yl)glycine (TZG) were purchased from Tocris (Bristol, UK). (R,S)-2-amino-2-(3-hydroxy-5-methylisoxazol-4-yl)acetic acid (AMAA) [16] and (R,S)-thioibotenic acid (thio-ibo) [17] were synthesized as previously described.

DNA constructs. For inducible expression in BHK-21 Tet-On cells, the open reading frame of rat NR1-1a (GenBank accession no. U11418) cDNA was subcloned into the pTRE2 vector (BD Biosciences Clontech, Heidelberg, Germany). For expression in *Xenopus* oocytes, NR1-1a cDNA was subcloned into the pCI-IRES-neo vector. The open reading frames of rat NR2A (D13211), NR2B (M91562), NR2C (D13212), and NR2D (D13214) cDNAs were subcloned into the pCI-IRES-bla vector. Constructs used for expression in *Xenopus* oocytes (pCI-IRES-neo and pCI-IRES-bla, containing a T7 site upstream from the 5' un-translated region) were linearized by restriction enzymes in order to produce cRNAs using mMessage mMachine kits (Ambion, Huntingdon, UK). The mammalian expression cassette of pCI-IRES-neo and pCI-IRES-bla contain (in the following order); a CMV enhancer/promoter region, a chimeric intron, a multiple cloning site, a synthetic intron, an internal ribosome entry site (IRES), neomycin phosphotransferase II gene (pCI-IRES-neo; G418-resistance) or blasticidin S deaminase gene (pCI-IRES-bla; blasticidin-resistance), and finally an SV40 late polyadenylation signal. Briefly, the NotI - NarI fragment of pIRESneo2 (BD Biosciences Clontech, Heidelberg, Germany) containing the synthetic intron and the IRES was subcloned into pCI-neo (Promega, Madison, WI), thereby producing the pCI-IRES-neo vector. The pCI-IRES-bla vector was produced by replacing the neomycin phosphotransferase II gene from pCI-IRES-neo with the blasticidin S deaminase gene from pcDNA6-E (Invitrogen, Carlsbad, CA).

Cell culturing and DNA transfection. BHK-21 cells were maintained at 37°C, 5% CO_2, and 95% relative humidity in DMEM containing GlutaMAX-I, 4500 mg/L glucose, and 110 mg/L sodium pyruvate (Invitrogen, Carlsbad, CA) supplemented with penicillin (100 units/mL), streptomycin (100 μg/mL), and 10% dialyzed fetal bovine serum (Invitrogen, Carlsbad, CA). All transfections were performed using Lipofectamine 2000 (Invitrogen, Carlsbad, CA). Six h after transfection, the medium was replaced by normal medium supplemented with 200 μM AP5 and 200 μM DCKA to prevent NMDA receptor-mediated cell death.

Generation of stable cell lines. In order to generate a Tet-On compatible cell line, BHK-21 cells were transfected with 5 μg pTet-On (BD Biosciences Clontech, Heidelberg, Germany) and clones resistant to 1 mg/mL G418 (Invitrogen, Carlsbad, CA) were selected. The monoclonal BHK-21 pTet-On stable cell line showing the lowest background and the highest doxycycline-induced (dox-induced) expression was selected according to the 'BD Tet-Off and Tet-On Gene Expression Systems User Manual' (BD Biosciences Clontech, Heidelberg, Germany) and used for generation of all the NMDA receptor cell lines. Transfection of BHK-21 pTet-On cells was performed using 20 μg NR1-1a pTRE2 together with 2 μg NR2A-D pCI-IRES-bla. The day after transfection, the cells were diluted 1:1000 and seeded in 144 mm dishes. The following day, 1 mg/mL G418 and 10 μg/mL blasticidin S (Sigma-Aldrich, Munich, Germany) were added to the medium. Unless otherwise noted, the medium always contained 1 mg/mL G418 and 10 μg/mL blasticidin S for selection, as well as 200 μM AP5 and 200 μM DCKA to prevent NMDA receptor-mediated cell death. G418-resistant and blasticidin S-resistant clones were isolated 10-14 days after transfection.

Intracellular calcium measurements using Fluo-4. In experiments using the fluometric imaging plate reader (FLIPR) (FLIPR^{384}; Molecular Devices, Sunnyvale, CA), cells were seeded into black-walled-clear-bottom 96-well plates at 20000 cells/well two days before the measurements. The culture medium was replaced one day before the assay with fresh medium or fresh medium containing 2 μg/mL dox to induce NR1-1a expression. On the day of the assay, cells were washed once in wash/load buffer containing (in mM): 1 probenecid (Sigma-Aldrich, Munich, Germany), 1.26 $CaCl_2$, 0.49 $MgCl_2$, 0.41 $MgSO_4$, 138 NaCl, 5.33 KCl, 0.34 Na_2HPO_4, 0.44 KH_2PO_4, 4.17 $NaHCO_3$, 5.56 D-glucose, and 20 HEPES pH 7.4. After this wash, the cells were loaded for 35 min at 37°C with 4.5 μM Fluo-4/AM (Molecular Probes Invitrogen, Carlsbad, CA) in wash/load buffer supplemented with 0.05% (w/v) Pluronic F-127 (solubility enhancer) (Molecular Probes Invitrogen, Carlsbad, CA). Cells were then washed two times in assay buffer containing (in mM): 10 $CaCl_2$, 138 NaCl, 5.33 KCl, 0.34 Na_2HPO_4, 0.44 KH_2PO_4, 4.17 $NaHCO_3$, 5.56 D-glucose, and 20 HEPES pH 7.4. After the last wash, 100 μL assay buffer was added to each well, and the cells were allowed to rest for 5 min at room temperature.

Fluorescence was measured using a FLIPR with excitation at 488 nm (argon-laser) and a 510-570 nm pass band emission filter. The baseline fluorescence (F_{basal}) of each 96-

well plate was set to approximately 10000 fluorescence units by adjusting the exposure length. F_{basal} was monitored for 20 s before applications were performed and fluorescence (F) in response to the application was measured for an additional 3-4 min. The volume of all applications was 25 µL and the ligand concentrations were added to the well (containing 100 µL assay buffer) at 5 times the final concentrations. Unless otherwise stated, 20 µM glycine (final concentration) was included in all applications except the buffer applications (controls). These control applications were used by the FLIPR software in order to correct for shift in baseline fluorescence caused by buffer addition to the wells. Usually, the shift was less than 5% of the maximal response elicited by glutamate (except for the NR1/NR2D cell line). Applications of 100 µM glutamate in order to determine maximal response and applications of 100 µM MK-801 in order to determine the level of basal activity were included on all 96-well plates. Furthermore, the fluorescence responses to all agonists could be completely inhibited by application of the open channel blocker MK-801, thereby demonstrating that none of the compounds display autofluorescence. The results are either displayed as fluorescence change = $F-F_{basal}$ or displayed as percentage (%) of baseline = 100% * F/F_{basal}, where F is the steady-state fluorescence signal measured after ligand application. Unless otherwise noted, all measurements were performed using 4-6 replicates (wells) and in at least 3 independent experiments.

Two-electrode voltage-clamp electrophysiology. Oocytes were surgically removed from mature female *Xenopus laevis* anaesthetized in 0.4% 3-aminobenzoic acid ethyl ester (Sigma-Aldrich, Munich, Germany) for 10-15 min. In order to remove the follicle layer, the oocytes were subsequently digested at room temperature for 3 h with 0.5 mg/mL collagenase (type IA; Sigma-Aldrich, Munich, Germany) in OR-2 buffer (in mM: 82.5 NaCl, 2.0 KCl, 1.0 $MgCl_2$, and 5.0 HEPES pH 7.6). The following day, healthy-looking stage V-VI oocytes were co-injected with cRNA encoding NR1-1a and the NR2 subunit at a 1:1 ratio and maintained at 18°C in Barth´s solution (in mM: 88 NaCl, 1.0 KCl, 2.4 $NaHCO_3$, 0.41 $CaCl_2$, 0.82 $MgSO_4$, 0.3 $Ca(NO_3)_2$, and 15 HEPES pH 7.6) supplemented with 100 IU/mL penicillin and 100 µg/mL streptomycin (Invitrogen, Carlsbad, CA).

TEVC recordings were performed at ambient temperatures 2-4 days after injection using an OC-725C Oocyte Clamp amplifier (Warner Instruments, Hampden, CT) with a Digidata 1322A interface (Molecular Devices, Sunnyvale, CA). The pClamp9 suite of programs (Molecular Devices, Sunnyvale, CA) was used for data acquisition. Currents were digitized at 100 Hz. The microelectrodes were fabricated from borosilicate glass capillaries (GC150TF-10, Harvard Apparatus, Holliston, MA) and pulled on a PC-10 puller (Narishige Instruments, Tokyo, Japan). Microelectrodes were filled with 3 M KCl and had 0.5-2.5 MΩ resistance. During recordings, the oocytes were voltage-clamped at -40 mV and continuously perfused with Ringer's solution containing (in mM) 115 NaCl, 2.5 KCl, 1.9 $BaCl_2$, and 10 HEPES (pH 7.6). The ligands were dissolved in Ringer's solution and applied to the oocytes by gravity-driven perfusion using a Valvebank 8 (Automate Scientific, San Francisco, CA). 20 µM glycine was included in the Ringer's solution at all times.

Data analysis. Data was analyzed with GraphPad Prism 4.0 (GraphPad Software, San Diego, CA). For concentration-response data obtained by $[Ca^{2+}]_i$ measurements, each data point was expressed as F/F_{basal} and averaged from 4-6 wells. These data points were fitted to the Hill equation: $F= F_{min} + ((F_{max} - F_{min})/(1 + 10\text{^}((\log EC_{50} - \log[A])* n_H)))$. F_{max} is the maximal response to the agonist, n_H denotes the Hill coefficient, [A] is the agonist concentration, and EC_{50} is the agonist concentration that produces half-maximal response. The $\log EC_{50}$ and n_H from the individual experiments were used to calculate the mean ± standard error of mean (SEM). For graphical presentation, a representative dataset ± standard deviation (SD) from an individual experiment was selected. The maximal response evoked by glutamate ($F_{max, glutamate}$) in the same experiment was normalized to 1 and the minimal response (F_{min}) was normalized to 0. The normalized data points were then fitted to the Hill equation and plotted together with the resulting curve. Relative F_{max} was calculated from a full concentration-response measurement as $(F_{max, agonist} - F_{min})/(F_{max, glutamate} - F_{min})$, where $F_{max, agonist}$ and F_{min} is the fitted values according to the Hill equation. Antagonist concentration-response data was calculated using a similar protocol, where instead of calculating the EC_{50}-value, the concentration required to inhibit a response evoked by 10 µM glutamate by 50% (IC_{50}) was calculated.

For electrophysiological recordings, agonist concentration-response data for individual oocytes were fitted to the Hill equation. The $\log EC_{50}$ and n_H from the individual oocytes were used to calculate the mean ± SEM. For graphical presentation, datasets from individual oocytes were normalized to the maximal response evoked by glutamate in the same recording. The mean ± SEM was calculated for each of the normalized data points. The averaged data points were then fitted to the Hill equation and plotted together with the resulting curve. Relative I_{max} was calculated from a full concentration-response measurement as $I_{max, agonist}/I_{max, glutamate}$, where $I_{max, agonist}$ is the fitted value according to the Hill equation and $I_{max, glutamate}$ is the maximal response evoked by glutamate in the same recording.

The two-tailed Pearson test for correlation was used to evaluate correlation between pEC_{50}-values or relative maximal responses obtained by $[Ca^{2+}]_i$ measurements and TEVC recordings.

RESULTS

Generation of cell lines with stable expression of NMDA receptor subtypes. To minimize cytotoxicity induced by NMDA receptor activation upon prolonged exposure to glutamate and glycine present in the culture medium, we decided to employ an inducible expression system. BHK-21 cells were transfected with the pTet-On plasmid and G418-resistant clones were isolated (See Materials and Methods). The resulting BHK-21 pTet-On stable cell lines constitutively express the "reverse" tetracycline-controlled transactivator that in the presence of doxycycline (dox) binds the tetracycline-response element and allows transcription of the gene encoded by the response plasmid.

The BHK-21 pTet-On cells were co-transfected with the response plasmid encoding NR1 controlled by the tetracycline-response element (NR1 pTRE2) and a plasmid encoding one of the four NR2 subunits and the blasticidin S-

resistance gene (NR2A-D pCI-IRES-bla). Cells were selected for G418-resistance and blasticidin S-resistance and clones expressing functional NMDA receptors were identified by $[Ca^{2+}]_i$ measurements. The functional expression of NMDA receptors were identified by $[Ca^{2+}]_i$ measurements both in the presence and absence of dox-induced expression of NR1. Glutamate (100 μM) was applied to determine the maximal response. To determine whether the glutamate-evoked response was specific for NMDA receptor activation, the response was inhibited by the open channel blocker MK-801 (100 μM) (data not shown). For some clones, application of MK-801 both inhibited the glutamate-evoked responses and the baseline fluorescence, indicating that there is basal activation of the NMDA receptors during the $[Ca^{2+}]_i$ measurements.

The clones showing high maximal responses assessed by application of glutamate (100 μM) and low levels of basal activation assessed by MK-801 (100 μM) were selected for further characterization. As shown in Fig. **1**, clones with no or very low basal NMDA receptor activation were isolated for the NR1/NR2A, NR1/NR2B, and NR1/NR2C cell lines, whereas all NR1/NR2D cell lines exhibited a basal activation.

In order to identify conditions with an optimal ratio between the glutamate-induced response and the level of basal activation $[Ca^{2+}]_i$ measurements were performed before and after dox-induction (data not shown). Surprisingly, a strong glutamate-induced $[Ca^{2+}]_i$ signal was observed for the NR1/NR2A, NR1/NR2B, and NR1/NR2C cell lines without dox-induction, suggesting that "leaky" transcription of the NR1 gene yields sufficient functional receptors despite the intended Tet-transcriptional control system. Dox-induction of NR1 expression at the NR1/NR2A, NR1/NR2B, and NR1/NR2C cell lines increased both the glutamate-induced response and the level of basal activation resulting in a lower ratio (data not shown). Dox-dependent induction of NR1 expression was necessary in order to obtain glutamate-induced responses at the NR1/NR2D cell line, but the glutamate-induced responses were still relatively small due to apparent high basal activation at the NR1/NR2D cell line (Fig. **1**). In order to maximize the glutamate-evoked responses and minimize the levels of basal activation, experiments with the NR1/NR2A, NR1/NR2B, and NR1/NR2C cell lines were subsequently performed without dox-induction.

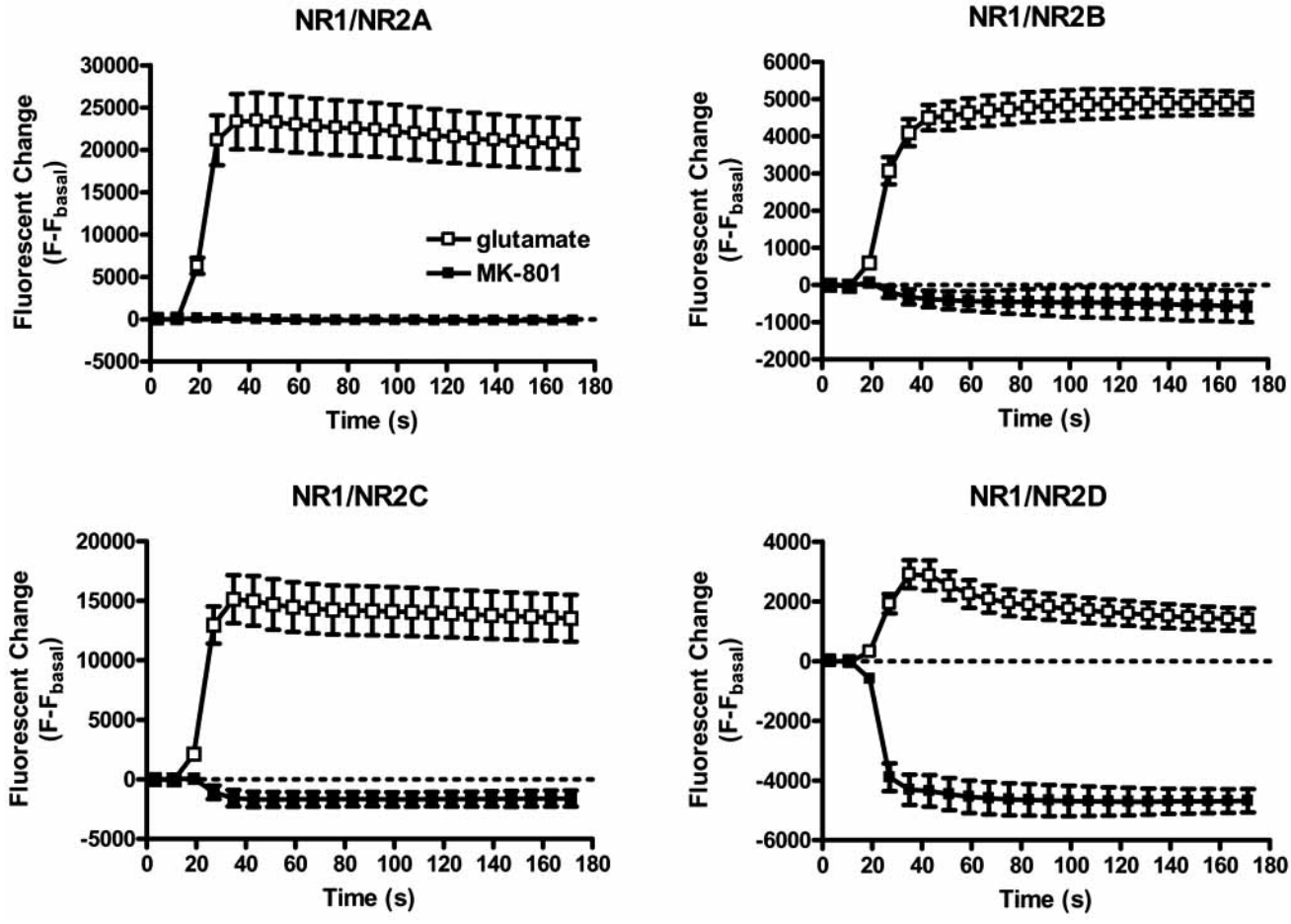

Fig. (1). Representative time-sequences of $[Ca^{2+}]_i$ measurements at four different cell lines with stable expression of NMDA receptor subtypes. Maximal response is determined by co-application of 100 μM glutamate and 20 μM glycine (□), and basal activation is determined by application of 100 μM MK-801 (■). The dotted line represents baseline fluorescence change. The results are displayed as $F\text{-}F_{basal}$, where F is the fluorescence measured after application of glutamate or MK-801. All data points are represented as mean ± SD of 4-6 wells.

Characterization of glutamate and glycine at NMDA receptor subtypes expressed in stable cell lines and in *Xenopus* oocytes. The utility of $[Ca^{2+}]_i$ measurements to characterize ligands at NMDA receptors expressed in stable cell lines depends on the ability of the assay to determine reliable and reproducible concentration-response data that correlate with results obtained using electrophysiological methods. We initially determined the concentration-response relationship for glutamate using $[Ca^{2+}]_i$ measurements at NMDA receptors expressed in the stable cell lines. The results were compared with corresponding data from characterization of glutamate using TEVC recordings at NMDA receptors expressed in *Xenopus* oocytes. The EC_{50}-values of glutamate (in the presence of 20 μM glycine) determined by TEVC recordings are 1.8-fold (NR1/NR2A), 2.2-fold (NR1/NR2B), 1.7-fold (NR1/NR2C), and 2.4-fold (NR1/NR2D) higher than those obtained by $[Ca^{2+}]_i$ measurements at the corresponding cell line (NR1/NR2A-D) (Fig. **2**, Tables **1** and **2**). The rank order of potencies for glutamate at the different NMDA receptor subtypes is the same in the two systems, namely NR1/NR2D > NR1/NR2C ≈ NR1/NR2B > NR1/NR2A.

Obtaining concentration-response data at the glycine site was more problematic, since co-application of 100 μM glutamate and 5 μM glycine elicited responses that were similar in magnitude to responses elicited by 100 μM glutamate alone without application of glycine (data not shown). Moreover, responses to co-application of 100 μM glutamate and 5 μM glycine were completely inhibited by excess of glycine-site antagonist (300 μM DCKA), suggesting that the

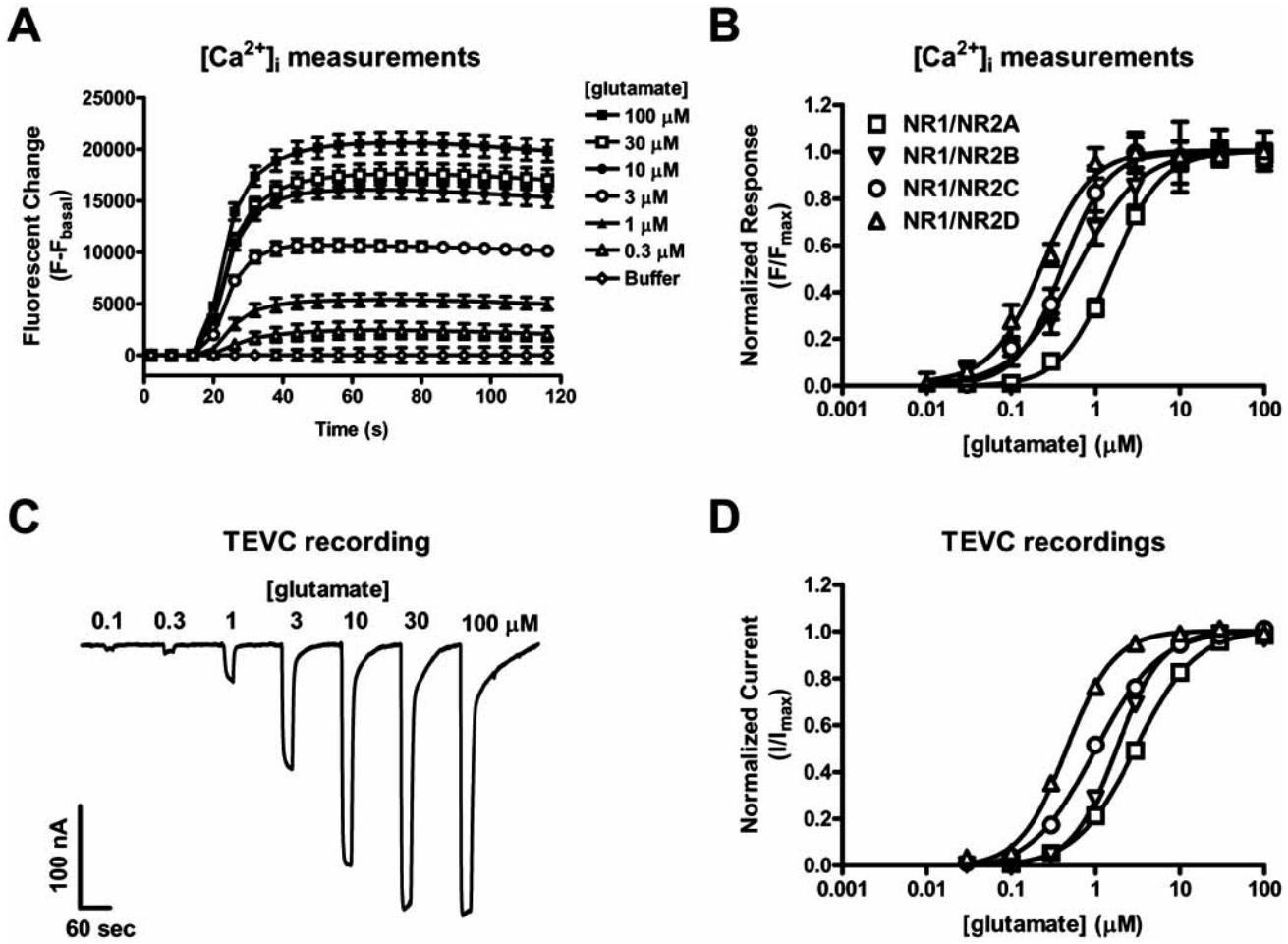

Fig. (2). (**A**) Representative time-sequences of fluorescence responses to increasing concentrations of glutamate (in the presence of 20 μM glycine) at the NR1/NR2A cell line. The data points are displayed as $F–F_{basal}$, where F is the fluorescence measured after application of glutamate or buffer. Data points are represented as mean ± SD of 4-6 wells. Concentration-dependent relaxations of response amplitudes were not observed and responses consistently reached steady-state plateaus. (**B**) Representative mean concentration-response curves for glutamate determined by $[Ca^{2+}]_i$ measurements at NMDA receptor subtypes expressed in stable cell lines. The maximal fluorescence response to glutamate (F_{max}) is normalized to 1, and the minimal response (F_{min}) is normalized to 0. Data points are represented as mean ± SD of 4-6 wells. (**C**) Representative current responses obtained from a TEVC recording on a *Xenopus* oocyte expressing NR1/NR2A receptors. Currents were evoked by application of glutamate at the concentration indicated above each response. (**D**) Mean concentration-response curves for glutamate determined by TEVC recordings at NMDA receptor subtypes expressed in *Xenopus* oocytes. The maximal current (I_{max}) in response to glutamate is normalized to 1. Glycine (20 μM) was included in all applications. Data points are represented as mean ± SEM of at least 3 oocytes. All EC_{50}-values are listed in Tables **1** and **2**.

glycine-site is saturated during the $[Ca^{2+}]_i$ measurements. Saturation of the glycine-site at the NR1 subunit has been reported previously for similar assay systems without continuous perfusion of the cells with assay buffer [8, 9]. Consequently, ligand characterization at the glycine site will require continuous perfusion as done during TEVC recordings on *Xenopus* oocytes. Concentration-response relationships for glycine at NMDA receptor subtypes were determined using TEVC recordings, and the rank order of potencies for glycine (in the presence of 30 μM glutamate) at the different NMDA receptor subtypes was NR1/NR2D > NR1/NR2C ≈ NR1/NR2B > NR1/NR2A (Table **1**).

Comparison of agonist concentration-response data determined by $[Ca^{2+}]_i$ measurements and TEVC recordings. In order to further evaluate the utility of the $[Ca^{2+}]_i$ measurements as a general approach to characterize agonists at NMDA receptors, we decided to compare agonist potencies and relative maximal responses obtained using $[Ca^{2+}]_i$ measurements with parallel data obtained using TEVC recordings on *Xenopus* oocytes. For this purpose, five glutamate-site agonists (aspartate, NMDA, AMAA, ibo, and thio-ibo; See Fig. **3A** for chemical structures) were characterized by $[Ca^{2+}]_i$ measurements at NR1/NR2A, NR1/NR2B, and NR1/NR2C receptors (Fig. **3B** and Table **2**) and by TEVC recordings at NR1/NR2A, NR1/NR2B, NR1/NR2C, and NR1/NR2D receptors (Table **1**). In general, aspartate is more potent than NMDA, and ibo is more potent than thio-ibo. At NR1/NR2A receptors, AMAA is more potent than NMDA. The highest selectivity was observed for aspartate by TEVC recordings being 9-fold more potent at NR1/NR2D compared to NR1/NR2A.

There was significant correlation (two-tailed Pearson test; see Materials and Methods) between pEC_{50}-values

Table 1. Pharmacological Characterization of Ligands at NMDA Receptors Expressed in *Xenopus* Oocytes (TEVC Recordings)

Agonist	NR1/NR2A		NR1/NR2B		NR1/NR2C		NR1/NR2D	
	EC_{50} (μM) [pEC_{50}]	**Relative I_{max}**	**EC_{50} (μM) [pEC_{50}]**	**Relative I_{max}**	**EC_{50} (μM) [pEC_{50}]**	**Relative I_{max}**	**EC_{50} (μM) [pEC_{50}]**	**Relative I_{max}**
(S)-glutamate	2.9 [5.53±0.08]	1	1.8 [5.75±0.03]	1	1.0 [5.99±0.05]	1	0.45 [6.34±0.03]	1
NMDA	75 [4.13±0.07]	0.90±0.04	22 [4.66±0.03]	0.77±0.01	23 [4.63±0.02]	0.73±0.02	8.3 [5.08±0.04]	0.80±0.02
(S)-aspartate	40 [4.40±0.02]	0.99±0.03	13 [4.89±0.01]	0.75±0.02	22 [4.66±0.01]	1.03±0.01	5.7 [5.24±0.01]	0.87±0.01
AMAA	31 [4.51±0.03]	0.09±0.01	45 [4.35±0.07]	0.58±0.02	40 [4.39±0.01]	0.36±0.01	15 [4.83±0.03]	0.72±0.02
ibo	40 [4.40±0.04]	0.68±0.07	27 [4.58±0.02]	0.76±0.04	39 [4.41±0.05]	0.66±0.02	17 [4.77±0.02]	0.78±0.01
thio-ibo	130 [3.88±0.04]	0.62±0.06	109 [3.96±0.02]	0.79±0.02	112 [3.95±0.02]	0.57±0.01	49 [4.31±0.05]	0.73±0.01
HQ[a]	16±5	-	26±3	-	56±5	-	75±4	-
glycine	1.2 [5.93±0.05]	-	0.16 [6.80±0.01]	-	0.17 [6.76±0.02]	-	0.069 [7.16±0.02]	-
Antagonist	**IC_{50} (μM) [pIC_{50}]**	**Estimated K_i (μM)**	**IC_{50} (μM) [pIC_{50}]**	**Estimated K_i (μM)**	**IC_{50} (μM) [pIC_{50}]**	**Estimated K_i (μM)**	**IC_{50} (μM) [pIC_{50}]**	**Estimated K_i (μM)**
AP5	0.39 [6.41±0.01]	0.09±0.01	2.8 [5.55±0.01]	0.43±0.01	5.9 [5.23±0.01]	0.54±0.02	21 [4.68±0.02]	0.91±0.01
(R)-CPP[b]	-	0.04±0.01	-	0.27±0.02	-	0.63±0.05	-	1.99±0.20
memantine[c]	4.36	-	1.2	-	0.601	-	0.820	-
PCP[c]	0.821	-	0.155	-	0.163	-	0.22	-
(+)-MK-801[c]	0.015	-	0.009	-	0.024	-	0.038	-
ifenprodil[d]	40	-	0.11	-	29	-	76	-

Parameters measured by TEVC recordings. Mean pEC_{50} ± SEM (shown in brackets) and the corresponding EC_{50}-values (in μM) as well as relative I_{max} ± SEM (relative to I_{max} of glutamate) were calculated from full concentration-response curves. For all agonist data, the Hill coefficients were between 1.1 and 1.8, and the number of oocytes was between 3 and 12.

Inhibition of NMDA receptor subtypes by increasing concentrations of AP5 was performed using 10 μM glutamate. The mean pIC_{50} ± SEM (shown in brackets) and the corresponding IC_{50}-value (in μM) were calculated from full concentration-response curves. For AP5, the Hill coefficients (n_H) were between -1.3 and -1.5 and the number of oocytes was 5. The estimated K_i-values were calculated from the corresponding IC_{50}-values according to the functional Cheng-Prusoff relationship [32]. The functional Cheng-Prusoff relationship use the assumption that $n_H = 1$ and the calculated K_i-values are therefore only estimates of the 'real' K_i-values that can be determined using Schild analysis [33, 34].

[a]Data from [35].

[b]Data from [18].

[c]Data from [19]; voltage-clamped at -40 mV.

[d]Data from [23]; human NMDA receptors.

Table 2. Pharmacological Characterization of Ligands at NMDA Receptors Expressed in BHK-21 Cells ($[Ca^{2+}]_i$ Measurements)

Agonist	NR1/NR2A		NR1/NR2B		NR1/NR2C		NR1/NR2D	
	EC_{50} (μM) [pEC_{50}]	Relative F_{max}	EC_{50} (μM) [pEC_{50}]	Relative F_{max}	EC_{50} (μM) [pEC_{50}]	Relative F_{max}	EC_{50} (μM) [pEC_{50}]	Relative F_{max}
(S)-glutamate	1.6 [5.78±0.10]	1	0.81 [6.09±0.07]	1	0.60 [6.22±0.06]	1	0.19 [6.72±0.11]	1
NMDA	22 [4.65±0.19]	0.69±0.10	13 [4.90± 0.06]	0.49±0.05	12 [4.92±0.02]	0.80±0.06	-	-
(S)-aspartate	11 [4.97±0.11]	0.96±0.02	5.4 [5.27±0.08]	0.51±0.01	3.7 [5.43±0.10]	0.84±0.02	-	-
AMAA	16 [4.81±0.21]	0.20±0.03	13 [4.88± 0.03]	0.51±0.05	15 [4.81± 0.06]	0.28±0.04	-	-
ibo	16 [4.79±0.15]	0.80±0.07	18 [4.75± 0.05]	0.64±0.04	14 [4.84±0.06]	0.55±0.01	-	-
thio-ibo	67 [4.17±0.13]	0.84±0.02	76 [4.12±0.08]	0.75±0.07	62 [4.21±0.06]	0.53±0.08	-	-
HQ	11 [4.97±0.05]	0.80±0.05	14 [4.84±0.02]	0.69±0.03	28 [4.56±0.07]	0.26±0.04	-	-
TZG	0.76 [6.12±0.01]	1.01±0.04	0.23 [6.64±0.05]	0.78±0.03	0.25 [6.60±0.06]	0.82±0.06	-	-
CCG	0.23 [6.65±0.15]	0.99±0.07	0.11 [6.96±0.11]	1.02±0.14	0.12 [6.91±0.02]	0.86±0.16	-	-
trans-ACBD	0.67 [6.18±0.03]	0.93±0.05	0.83 [6.08±0.04]	0.75±0.01	1.1 [5.97±0.09]	0.56±0.09	-	-
cis-ACPD	16 [4.78±0.09]	0.76±0.03	24 [4.62±0.10]	0.71±0.03	16 [4.80±0.02]	0.50±0.03	-	-
Antagonist	**IC_{50} (μM) [pIC_{50}]**	**Estimated K_i (μM)**	**IC_{50} (μM) [pIC_{50}]**	**Estimated K_i (μM)**	**IC_{50} (μM) [pIC_{50}]**	**Estimated K_i (μM)**	**IC_{50} (μM) [pIC_{50}]**	**Estimated K_i (μM)**
AP5	5.8 [5.23±0.03]	0.88±0.26	43 [4.37±0.05]	2.7±0.3	80 [4.10±0.05]	4.2±0.3	-	-
(R)-CPP	0.55 [6.26±0.07]	0.07±0.01	3.2 [5.50±0.06]	0.22±0.04	14 [4.84±0.03]	0.78±0.08	-	-
LY235959	0.34 [6.47±0.06]	0.032±0.003	0.48 [6.32±0.01]	0.031±0.009	0.48 [6.32±0.03]	0.022±0.003	-	-
memantine	11 [4.96±0.05]	-	2.0 [5.71±0.11]	-	1.9 [5.71±0.07]	-	-	-
PCP	1.4 [5.85±0.08]	-	0.31 [6.51±0.27]	-	1.9 [5.73±0.20]	-	-	-
(+)-MK-801	0.16 [6.79±0.09]	-	0.12 [6.92±0.12]	-	0.95 [6.02±0.09]	-	-	-
ifenprodil	419 [3.38±0.06]	-	0.52 [6.28±0.05]	-	260 [3.59±0.07]	-	-	-

Parameters measured by $[Ca^{2+}]_i$ measurements. Mean pEC_{50} ± SEM (shown in brackets) and the corresponding EC_{50}-values (in μM) as well as relative F_{max} ± SEM (relative to F_{max} of glutamate) were calculated from full concentration-response curves. For all agonist data, the Hill coefficients were between 1.0 and 1.8, and the number of experiments was between 3 and 6. Inhibition of NMDA receptor subtypes by increasing concentrations of antagonist was performed using 10 μM glutamate. Mean pIC_{50} ± SEM (shown in brackets) and the corresponding IC_{50}-values (in μM) were calculated from full concentration-response curves. The Hill coefficients were between -0.8 and -1.9 and the number of oocytes 3 or 4. The IC_{50} and glutamate EC_{50} obtained in one individual experiment were used to calculate the estimated K_i-values according to the functional Cheng-Prusoff relationship [32], and the estimated K_i-values of all experiments were used to calculate the mean estimated K_i ± SEM. The functional Cheng-Prusoff relationship use the assumption that $n_H = 1$ and the calculated K_i-values are therefore only estimates of the 'real' K_i-values that can be determined using Schild analysis [33, 34].

determined by $[Ca^{2+}]_i$ measurements and TEVC recordings with the following coefficients of determination: $r^2 = 0.95$ at NR1/NR2A ($P < 0.01$), $r^2 = 0.95$ at NR1/NR2B ($P < 0.01$), and $r^2 = 0.92$ at NR1/NR2C ($P < 0.01$). However, there was a tendency that the EC_{50}-values determined by $[Ca^{2+}]_i$ measurements were lower than the corresponding EC_{50}-values determined by TEVC recordings (Fig. **4A**).

Significant correlation between relative maximal responses determined by $[Ca^{2+}]_i$ measurements and TEVC recordings was observed for NR1/NR2A ($r^2 = 0.78$; $P < 0.05$) and NR1/NR2C ($r^2 = 0.85$; $P < 0.05$), but not for NR1/NR2B ($r^2 = 0.22$). This may be explained by the fact that the relative maximal responses determined at NR1/NR2B receptors lie within a narrow range compared to those determined at NR1/NR2A and NR1/NR2C receptors (Fig. **4B**).

Characterization of antagonists at NMDA receptor subtypes. For a more general characterization, three competitive antagonists acting at the glutamate-site and three channel blockers were characterized at the NR1/NR2A, NR1/NR2B, and NR1/NR2C cell lines. Characterization of competitive antagonists revealed the following rank order of potencies at NR1/NR2B and NR1/NR2C receptors: LY235959 > CPP > AP5, whereas at LY235959 and CPP were equipotent at NR1/NR2A receptors (LY235959 ≈ CPP > AP5) (Fig. **5A** and Table **2**). The rank order of potencies for AP5 and CPP is NR1/NR2A > NR1/NR2B > NR1/NR2C, whereas LY235959 is equally potent at these NMDA receptor subtypes. The rank orders of potencies for AP5 and CPP obtained by $[Ca^{2+}]_i$ measurements are similar to those determined by TEVC recordings (Table **1**). The IC_{50}-values of AP5 determined by $[Ca^{2+}]_i$ measurements are

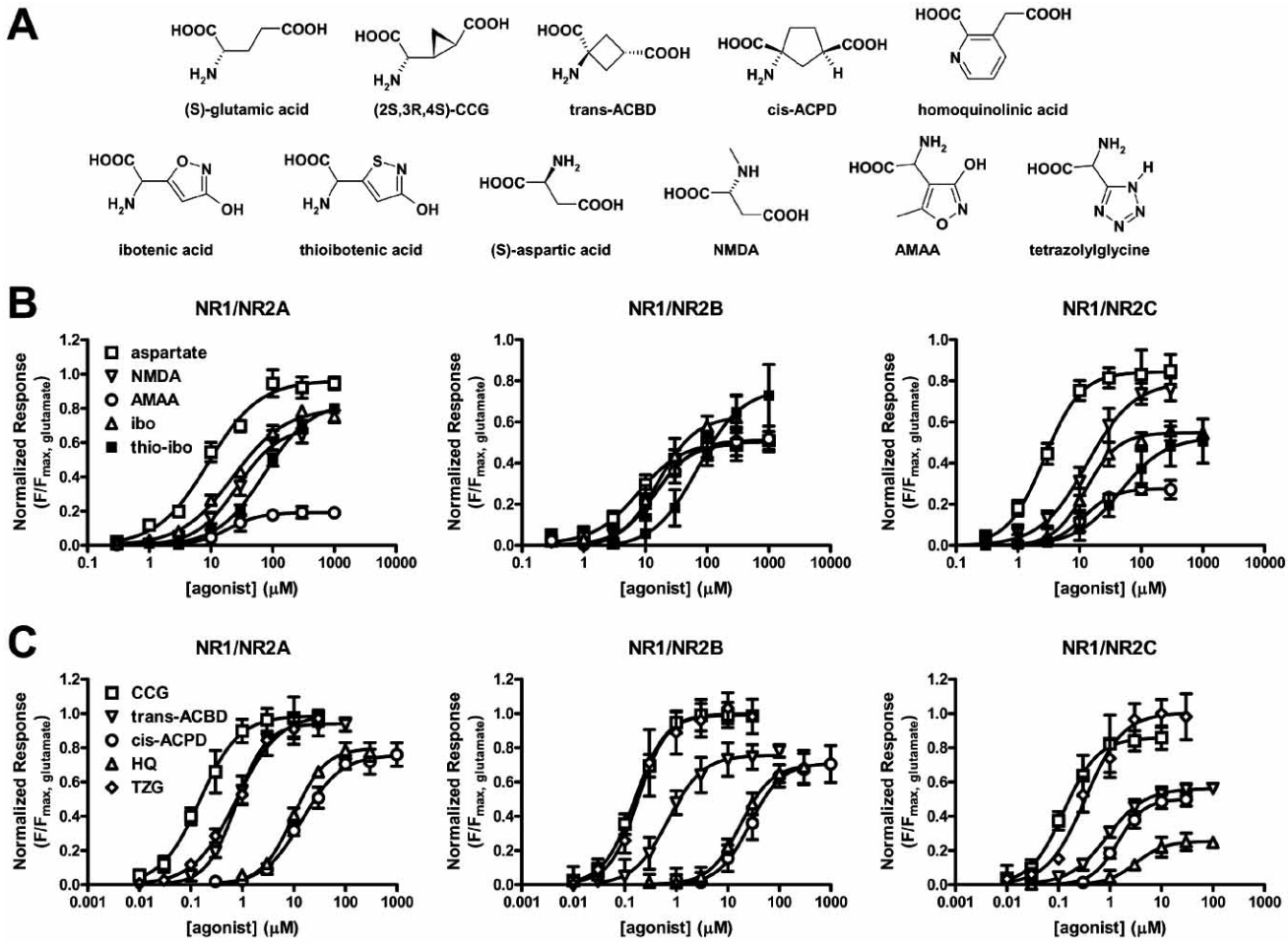

Fig. (3). (**A**) Chemical structures of agonists characterized at recombinant NMDA receptors in the present study. The depicted structure of cis-ACPD is the NMDA receptor-selective enantiomer (1R,3R)-1-aminocyclopentane-cis-1,3-dicarboxylic acid, but the cis-ACPD characterized in this study is a 1:1 mixture of the (1R,3R)-enantiomer and the (1S,3S)-enantiomer. Ibotenic acid (ibo), thioibotenic acid (thio-ibo), AMAA, and tetrazolylglycine (TZG) are characterized as racemates. The depicted structures are the fully protonated and uncharged forms of the ligands. (**B**) Representative mean concentration-response curves for aspartate, NMDA, AMAA, ibo, and thio-ibo determined by $[Ca^{2+}]_i$ measurements at NR1/NR2A (left), NR1/NR2B (middle), and NR1/NR2C (right) receptors expressed in stable cell lines. (**C**) Representative mean concentration-response curves for CCG, trans-ACBD, cis-ACPD, HQ, and TZG determined by $[Ca^{2+}]_i$ measurements at NR1/NR2A (left), NR1/NR2B (middle), NR1/NR2C (right) receptors expressed in stable cell lines. The maximal fluorescence response to glutamate ($F_{max, glutamate}$) is normalized to 1, and the minimal response (F_{min}) is normalized to 0. The fluorescence responses to the agonists are normalized to $F_{max, glutamate}$. Data points are represented as mean ± SD of 4-6 wells. The EC_{50}-values are listed in Table **2**.

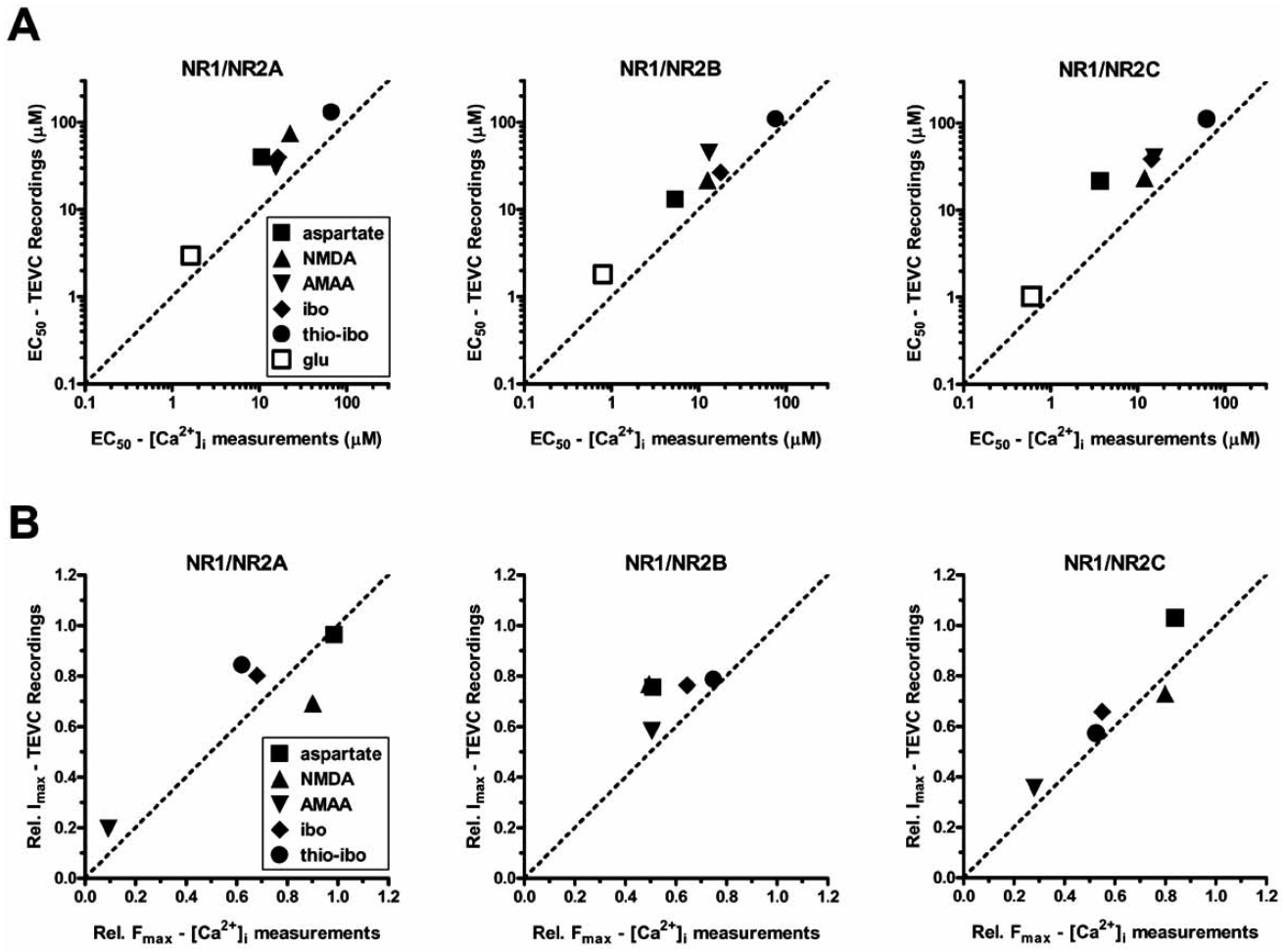

Fig. (4). (**A**) Correlation between EC_{50}-values of agonists at NR1/NR2A (left), NR1/NR2B (middle), NR1/NR2C (right) receptors determined by $[Ca^{2+}]_i$ measurements and TEVC recordings. EC_{50}-values are listed in Tables **1** and **2**. The dotted line represents a situation where the EC_{50}-value determined by $[Ca^{2+}]_i$ measurements is identical to the corresponding EC_{50}-value determined by TEVC recordings. (**B**) Correlation between relative maximal responses of agonists at NR1/NR2A (left), NR1/NR2B (middle), NR1/NR2C (right) receptors determined by $[Ca^{2+}]_i$ measurements and TEVC recordings. The relative I_{max}-values are listed in Table **1** and the relative F_{max}-values are listed in Table **2**. The dotted line represents a situation where the relative F_{max} determined by $[Ca^{2+}]_i$ measurements is identical to the corresponding relative I_{max} determined by TEVC recordings.

14- to 15-fold higher than those obtained by TEVC recordings, and the corresponding estimated K_i-values are 6.3- to 9.8-fold higher. On the other hand, our estimated K_i-values for CPP determined by $[Ca^{2+}]_i$ measurements are in agreement with those determined in a previous study by TEVC recordings [18]. LY235959 has not previously been characterized at recombinant NMDA receptors.

Memantine, PCP, and MK-801 are open channel blockers that inhibit NMDA receptors in a voltage- and use-dependent manner [19, 20]. Previous studies have characterized memantine [19-21], PCP [19] and MK-801 [19, 22] by TEVC recordings. We have characterized memantine, PCP, and MK-801 by $[Ca^{2+}]_i$ measurements at NR1/NR2A, NR1/NR2B, and NR1/NR2C receptors (Fig. **5B** and Table **2**). MK-801 is ~10-fold and memantine and PCP were ~2-fold more potent at inhibiting NR1/NR2A and NR1/NR2B receptors when characterized by TEVC recordings (Table **1**) than by $[Ca^{2+}]_i$ measurements (Table **2**). At NR1/NR2C receptors, these differences were 3.2-, 11-, and 40-fold for memantine, PCP, and MK-801, respectively. These discrepancies are likely a result of differences in membrane potentials, since the TEVC recordings are performed under voltage-clamped conditions. Although the cells are not voltage-clamped during $[Ca^{2+}]_i$ measurements, saturating concentrations of memantine, PCP, or MK-801 were able to consistently inhibit glutamate-evoked responses by 100% (data not shown).

The IC_{50}-values of the NR2B-selective non-competitive antagonist ifenprodil have previously been determined by TEVC recordings at human NMDA receptors to be 360-fold and 260-fold higher at NR1/NR2A and NR1/NR2C receptors, respectively, relative to at NR1/NR2B receptors (Table **1**) [23]. Using $[Ca^{2+}]_i$ measurements, the IC_{50}-values of ifenprodil at rat NMDA receptors are 800-fold and 500-fold higher at NR1/NR2A and NR1/NR2C receptors, respectively, relative to those at NR1/NR2B receptors (Table **2**). These data confirm the subtype-selectivity of ifenprodil and demonstrate that the stable cell lines in conjunction with

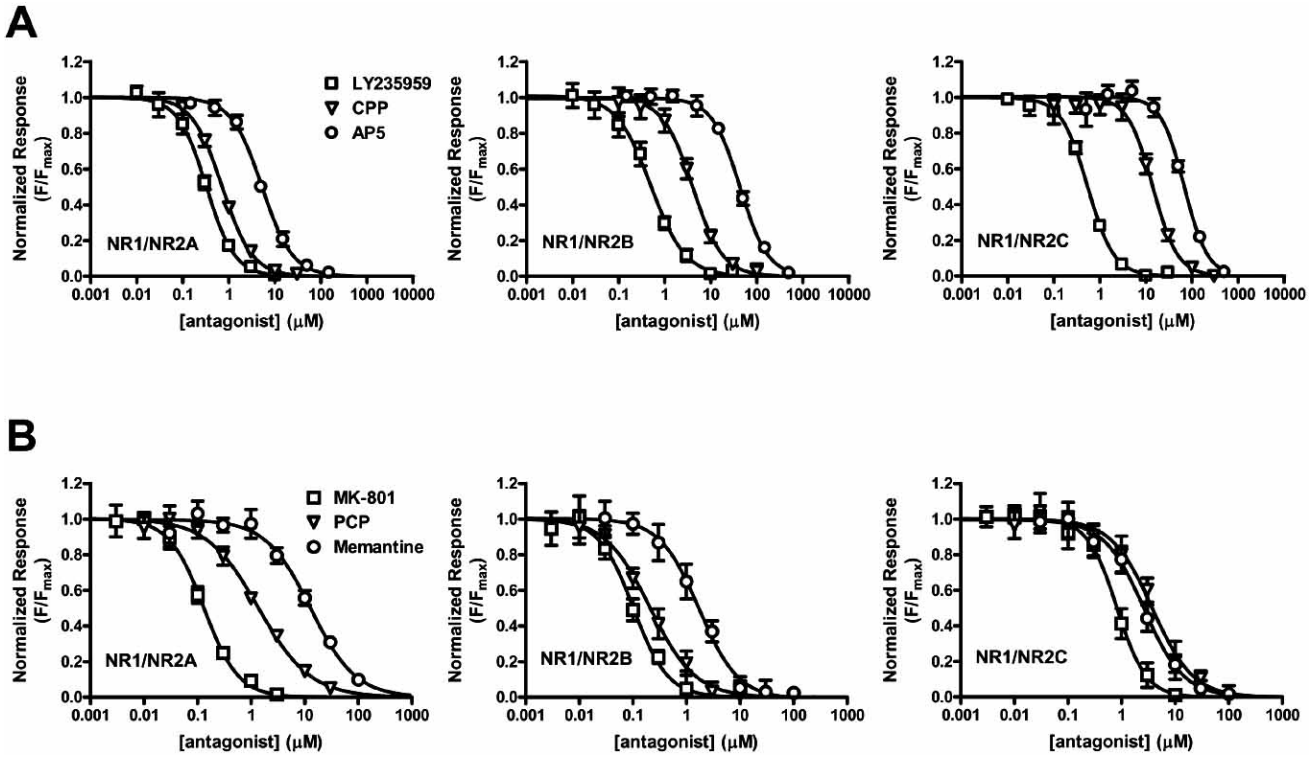

Fig. (5). (A) Representative mean concentration-response curves for inhibition of glutamate-evoked responses by competitive antagonists determined by $[Ca^{2+}]_i$ measurements at NR1/NR2A (left), NR1/NR2B (middle), and NR1/NR2C (right) receptors expressed in stable cell lines. (**B**) Representative mean concentration-response curves for inhibition of glutamate-evoked responses by channel blockers determined by $[Ca^{2+}]_i$ measurements at NR1/NR2A (left), NR1/NR2B (middle), and NR1/NR2C (right) receptors expressed in stable cell lines. The responses were evoked by co-application of 10 μM glutamate and 20 μM glycine. Data points are represented as mean ± SD of 4-6 wells. The IC_{50}-values are listed in Table **2**.

$[Ca^{2+}]_i$ measurements can be used to identify and characterize subtype-selective NMDA receptor antagonists.

Characterization of agonists at NMDA receptor subtypes expressed in stable cell lines. In order to identify potential subtype-selectivity among known NMDA receptor agonists, we expanded the characterization of agonists with three conformationally constrained analogues of glutamate, namely CCG, trans-ACBD, and cis-ACPD, as well as TZG, which are potent and NMDA receptor-selective agonists that previously have been characterized by binding and electrophysiology at native NMDA receptors [24-27] and recently also using TEVC recordings [28]. We characterized these agonists as well as another conformationally constrained analogue of glutamate, namely HQ, at NR1/NR2A, NR1/NR2B, and NR1/NR2C receptors using $[Ca^{2+}]_i$ measurements (Fig. **3C** and Table **2**). Chemical structures are shown in Fig. **3A**.

The pharmacological characterization of the agonists confirms the results obtained at native NMDA receptors regarding agonist potencies. CCG and TZG are more potent than glutamate at all the characterized NMDA receptor subtypes, and glutamate and trans-ACBD are in general equally potent. The observed selectivity profile for HQ in the $[Ca^{2+}]_i$ assay (NR1/NR2A ≥ NR1/NR2B ≥ NR1/NR2C) (Table **2**) has been confirmed by others using TEVC recordings (Table **1**). However, subtype-selectivity was not observed for any of the characterized agonists. The highest selectivity was observed for TZG being ~3-fold more potent at NR1/NR2B and NR1/NR2C compared to NR1/NR2A.

DISCUSSION

Expression system for stable NMDA receptor-expressing cell lines. When expressing NMDA receptors in mammalian cell lines, the major obstacle is to obtain sufficient expression levels to perform the relevant assays without causing NMDA receptor-mediated cytotoxicity. To overcome this obstacle, we took three precautions. First, the culture medium was supplemented with two NMDA receptor antagonists acting at the glutamate-site and glycine-site, respectively. Second, an expression system with inducible expression of the NR1 subunit and constitutive expression of the NR2 subunit was utilized to reduce the number of functional NMDA receptors present during maintenance of the cell lines. Finally, the BHK-21 cell line endogenously express transport system for high affinity uptake of glutamate and aspartate [29], and therefore, this cell line was used as parental cell line in order to reduce glutamate and aspartate in the culture medium. The majority of the previously described cell lines with stable expression of NMDA receptors have been cultured in the presence of the open channel blocker ketamine in order to prevent cytotoxicity [6-9, 11, 12]. Although ketamine is an uncompetitive antagonist and therefore offers effective blockade of the NMDA receptors independent of agonist concentration, the usage of open

channel blockers raises concern related to the slow dissociation rate of these compounds and the possibility that bound channel blocker may interfere with the functional assay. The cell lines presented in this study are cultured in the presence of the glutamate-site antagonist AP5 and the glycine-site antagonist DCKA. These competitive antagonists are readily washed out prior to the functional assay, but their capacity to inhibit the expressed NMDA receptors is also more sensitive to the concentrations of glutamate/aspartate and glycine in the culture medium. However, build-up of glutamate and aspartate concentrations will be limited by the endogenous transporters of the BHK-21 cells.

It was not necessary to induce expression of the NR1 subunit before performing $[Ca^{2+}]_i$ measurements with the three stable cell lines expressing NR1/NR2A, NR1/NR2B, or NR1/NR2C receptors, suggesting that "leaky" expression of the NR1 subunit provide a suitable balance between NMDA receptor expression levels and cytotoxicity. By contrast, induction of NR1 expression was required for detectable expression of the NR1/NR2D receptors. A reasonable explanation to the observed dependencies on NMDA receptor expression levels for the individual cell lines could be that the balance between these levels and cytotoxicity is determined by the properties of the expressed NR2 subunit. The EC_{50} of glutamate is 6.4-fold higher at NR1/NR2A receptors relative to at NR1/NR2D receptors (determined by TEVC recordings), and the order of glutamate potencies is NR1/NR2D > NR1/NR2C ≈ NR1/NR2B > NR1/NR2A, making the NR1/NR2D cell line most sensitive to contaminating glutamate in the culture medium or assay buffer.

Clones showing low levels of basal activation were selected for the cell lines expressing NR1/NR2A, NR1/NR2B, and NR1/NR2C receptors. Despite considerable effort, it was not possible to isolate NR1/NR2D receptor-expressing clones with low basal activation, suggesting that the basal activation is due to the presence of contaminating glutamate/aspartate and glycine in the assay buffer. BHK-21 cells are known to contain a large pool of intracellular glutamate [29], and studies on metabotropic glutamate receptors expressed in BHK-21 cells have demonstrated that glutamate can be extruded within minutes after wash with assay buffer [30]. Given the order of glutamate potencies at the NMDA receptor subtypes (NR1/NR2A-D), this will generate the highest levels of basal activation at clones expressing NR1/NR2D receptors. Only very low levels of basal activation were detected for the cell lines expressing NR1/NR2A, NR1/NR2B, and NR1/NR2C receptors (Fig. **1**), and we therefore argue that any potential presence of contaminating glutamate/aspartate in the assay buffer is not affecting the characterization of ligands at these expressed NMDA receptor subtypes.

Evaluation of concentration-response data obtained at recombinant NMDA receptors. We compared concentration-response data obtained by $[Ca^{2+}]_i$ measurements with data obtained by TEVC recordings in order to evaluate the utility of $[Ca^{2+}]_i$ measurements to characterize ligands at NMDA receptors expressed in stable cell lines. With respect to competitive antagonists, only concentration-response data for AP5 were compared in this way and we are therefore unable to conclude whether the $[Ca^{2+}]_i$ measurements at the NMDA receptor cell lines can reliably report on competitive antagonist pharmacology. With respect to agonists, there was good correlation between the EC_{50}-values determined by the two assays, although the EC_{50}-values determined by $[Ca^{2+}]_i$ measurements were marginally lower than those determined by TEVC recordings. The difference could suggest saturation of the $[Ca^{2+}]_i$ signal at non-maximal concentrations. However, the good correlation between the maximal responses determined by the two methods makes this a less likely explanation. It is possible that the observed differences in the measured EC_{50}-values are simply explained by the marked differences that exist between the two heterologous expression systems (BHK-21 *vs Xenopus* oocytes) and the two functional assays ($[Ca^{2+}]_i$ measurements *vs* TEVC recordings).

Eleven agonists, three competitive antagonists, three open channel blockers, and one non-competitive antagonist were characterized using $[Ca^{2+}]_i$ measurements. However, this fluorescence-based assay, which is an indirect measurement of NMDA receptor function, is sensitive to several potential problems, such as intracellular buffering or sequestration of $[Ca^{2+}]_i$, differences in dye loading efficiency, and autofluorescence by cellular constituents or the ligand itself [31]. Nevertheless, based on the concentration-response data of the ligands at the stable cell lines and the observed correlation with parallel data obtained by direct measurements of receptor function (TEVC recordings), it appears that potential artifacts of the fluorescence-based readout have only minor, if any, influence on the reported pharmacology of the ligands.

CONCLUSION

In the present study, we describe a general approach to establish cell lines with stable expression of NMDA receptor subtypes. Furthermore, we characterize a range of ligands at different NMDA receptor subtypes expressed in stable cell lines and in *Xenopus* oocytes using either $[Ca^{2+}]_i$ measurements or TEVC recordings, respectively. These data represent a comprehensive characterization of ligands at recombinant NMDA receptor subtypes and demonstrate that stable NMDA receptor-expressing cell lines can be used to generate reliable concentration-response data for agonists acting at the glutamate binding site of NR1/NR2A, NR1/NR2B, and NR1/NR2C NMDA receptor subtypes. Although the utility of stable cell lines to report on the pharmacology of the NR1/NR2D subtype and ligands acting at the glycine binding site may be less reliable, these data show that assays using fluorescence measurements provide a valuable approach for understanding of drug actions at NMDA receptors. By sharing knowledge of steps and considerations important for generation of stable cell lines expressing NMDA receptors, we have provided a basis for high throughput screening as well as pharmacological characterization of NMDA receptors.

ACKNOWLEDGEMENTS

We thank Dr. Ulf Madsen for generously supplying us with (RS)-AMAA. We also thank Prof. Shigetada Nakanishi for sharing the NMDA receptor cDNAs. The authors would like to acknowledge Dr. Anders A. Jensen for helpful discussions and commentary on the project. This work was sup-

ported by the Novo Nordisk Foundation, the Villum Kann Rasmussen Foundation, and the Lundbeck Foundation.

ABBREVIATIONS

AMAA	=	(R,S)-2-Amino-2-(3-hydroxy-5-methyl-isoxazol-4-yl)acetic acid
AP5	=	(R,S)-2-Amino-5-phosphonopentanoic acid
CCG	=	(2S,3R,4S)-α-(Carboxycyclopro-pyl)glycine
cis-ACPD	=	(±)-1-Aminocyclopentane-r-1,cis-3-dicar-boxylic acid
CPP	=	(R)-4-(3-Phosphonopropyl)piperazine-2-carboxylic acid
DCKA	=	5,7-Dichlorokynurenic acid
dox	=	Doxycycline
FLIPR	=	Fluometric imaging plate reader
HQ	=	Homoquinolinic acid
ibo	=	(R,S)-Ibotenic acid
NMDA	=	N-Methyl-D-aspartate
PCP	=	Phencyclidine
TEVC	=	Two-electrode voltage-clamp
thio-ibo	=	(R,S)-Thioibotenic acid
trans-ACBD	=	1-Aminocyclobutane-r-1,cis-3-dicar-boxylic acid
TZG	=	(R,S)-(Tetrazol-5-yl)glycine

REFERENCES

[1] Dingledine, R.; Borges, K.; Bowie, D.; Traynelis, S.F. *Pharmacol. Rev.*, **1999**, *51*, 7.

[2] Bräuner-Osborne, H.; Egebjerg, J.; Nielsen, E.Ø.; Madsen, U.; Krogsgaard-Larsen, P. *J. Med. Chem.*, **2000**, *43*, 2609.

[3] Nishi, M.; Hinds, H.; Lu, H.P.; Kawata, M.; Hayashi, Y. *J. Neurosci.*, **2001**, *21*, RC185.

[4] Boeckman, F.A.; Aizenman, E. *Neurosci. Lett.*, **1994**, *173*, 189.

[5] Monyer, H.; Sprengel, R.; Schoepfer, R.; Herb, A.; Higuchi, M.; Lomeli, H.; Burnashev, N.; Sakmann, B.; Seeburg, P.H. *Science*, **1992**, *256*, 1217.

[6] Grimwood, S.; Le, B.B.; Atack, J.R.; Barton, C.; Cockett, W.; Cook, S.M.; Gilbert, E.; Hutson, P.H.; McKernan, R.M.; Myers, J.; Ragan, C.I.; Wingrove, P.B.; Whiting, P.J. *J Neurochem.*, **1996**, *66*, 2239.

[7] Priestley, T.; Laughton, P.; Myers, J.; Le, B.B.; Kerby, J.; Whiting, P.J. *Mol. Pharmacol.*, **1995**, *48*, 841.

[8] Steinmetz, R.D.; Fava, E.; Nicotera, P.; Steinhilber, D. *J. Neurosci. Methods*, **2002**, *113*, 99.

[9] Varney, M.A.; Jachec, C.; Deal, C.; Hess, S.D.; Daggett, L.P.; Skvoretz, R.; Urcan, M.; Morrison, J.H.; Moran, T.; Johnson, E.C.; Velicelebi, G. *J. Pharmacol. Exp. Ther.*, **1996**, *279*, 367.

[10] Uchino, S.; Watanabe, W.; Nakamura, T.; Shuto, S.; Kazuta, Y.; Matsuda, A.; Nakajima-Iijima, S.; Kudo, Y.; Kohsaka, S.; Mishina, M. *FEBS Lett.*, **2001**, *506*, 117.

[11] Kurko, D.; Dezso, P.; Boros, A.; Kolok, S.; Fodor, L.; Nagy, J.; Szombathelyi, Z. *Neurochem. Int.*, **2005**, *46*, 369.

[12] Nagy, J.; Boros, A.; Dezso, P.; Kolok, S.; Fodor, L. *Neurochem. Int.*, **2003**, *43*, 19.

[13] Renard, S.; Drouet-Petre, C.; Partiseti, M.; Langer, S.Z.; Graham, D.; Besnard, F. *Eur. J. Pharmacol.*, **1999**, *366*, 319.

[14] Boeckman, F.A.; Aizenman, E. *J. Pharmacol. Exp. Ther.*, **1996**, *279*, 515.

[15] Cik, M.; Chazot, P.L.; Stephenson, F.A. *Biochem. J.*, **1993**, *296*, 877.

[16] Madsen, U.; Ferkany, J.W.; Jones, B.E.; Ebert, B.; Johansen, T.N.; Holm, T.; Krogsgaard-Larsen, P. *Eur. J. Pharmacol.*, **1990**, *189*, 381.

[17] Bunch, L.; Krogsgaard-Larsen, P.; Madsen, U. *J. Org. Chem.*, **2002**, *67*, 2375.

[18] Feng, B.; Tse, H.W.; Skifter, D.A.; Morley, R.; Jane, D.E.; Monaghan, D.T. *Br. J. Pharmacol.*, **2004**, *141*, 508.

[19] Dravid, S.M.; Erreger, K.; Yuan, H.; Nicholson, K.; Le, P.; Lyuboslavsky, P.; Almonte, A.; Murray, E.; Mosely, C.; Barber, J.; French, A.; Balster, R.; Murray, T.F.; Traynelis, S.F. *J. Physiol.*, **2007**, *581*, 107.

[20] Parsons, C.G.; Gruner, R.; Rozental, J.; Millar, J.; Lodge, D. *Neuropharmacology*, **1993**, *32*, 1337.

[21] Parsons, C.G.; Danysz, W.; Bartmann, A.; Spielmanns, P.; Frankiewicz, T.; Hesselink, M.; Eilbacher, B.; Quack, G. *Neuropharmacology*, **1999**, *38*, 85.

[22] Monaghan, D.T.; Larsen, H. *J. Pharmacol. Exp. Ther.*, **1997**, *280*, 614.

[23] Hess, S.D.; Daggett, L.P.; Deal, C.; Lu, C.C.; Johnson, E.C.; Velicelebi, G. *J. Neurochem.*, **1998**, *70*, 1269.

[24] Shinozaki, H.; Ishida, M.; Shimamoto, K.; Ohfune, Y. *Brain Res.*, **1989**, *480*, 355.

[25] Allan, R.D.; Hanrahan, J.R.; Hambley, T.W.; Johnston, G.A.; Mewett, K.N.; Mitrovic, A.D. *J. Med. Chem.*, **1990**, *33*, 2905.

[26] Curry, K.; Peet, M.J.; Magnuson, D.S.; McLennan, H. *J. Med. Chem.*, **1988**, *31*, 864.

[27] Schoepp, D.D.; Smith, C.L.; Lodge, D.; Millar, J.D.; Leander, J.D.; Sacaan, A.I.; Lunn, W.H. *Eur. J. Pharmacol.*, **1991**, *203*, 237.

[28] Erreger, K.; Geballe, M.T.; Kristensen, A.; Chen, P.E.; Hansen, K.B.; Lee, C.J.; Yuan, H.; Le, P.; Lyuboslavsky, P.N.; Micale, N.; JØrgensen, L.; Clausen, R.P.; Wyllie, D.J.; Snyder, J.P.; Traynelis, S.F. *Mol. Pharmacol.*, **2007**, *72*, 907.

[29] Scott, D.M.; Pateman, J.A. *Biochim. Biophys. Acta*, **1978**, *508*, 379.

[30] Thomsen, C.; Hansen, L.; Suzdak, P.D. *J. Neurochem.*, **1994**, *63*, 2038.

[31] Takahashi, A.; Camacho, P.; Lechleiter, J.D.; Herman, B. *Physiol. Rev.*, **1999**, *79*, 1089.

[32] Craig, D.A. *Trends Pharmacol. Sci.*, **1993**, *14*, 89.

[33] Frizelle, P.A.; Chen, P.E.; Wyllie, D.J. *Mol. Pharmacol.*, **2006**, *70*, 1022.

[34] Wyllie, D.J.; Chen, P.E. *Br. J. Pharmacol.*, **2007**, *150*, 541.

[35] Buller, A.L.; Monaghan, D.T. *Eur. J. Pharmacol.*, **1997**, *320*, 87.

Received: September 14, 2007 **Revised: November 6, 2007** **Accepted: November 28, 2007**